

Proton-Coupled Photoinduced Electron Transfer, Deuterium Isotope Effects, and Fluorescence Quenching in Noncovalent Benzo[*a*]pyrenetetraol–Nucleoside Complexes in Aqueous Solutions

Vladimir Ya. Shafirovich,[†] Scott H. Courtney, Naiqi Ya, and Nicholas E. Geacintov*

Contribution from the Chemistry Department and Radiation and Solid State Laboratory, 31 Washington Place, New York University, New York, New York 10003

Received November 3, 1994[⊗]

Abstract: A proton-coupled, photoinduced electron transfer mechanism is responsible for the extraordinarily efficient dynamic and static quenching (94–99%) of the fluorescence of the pyrenyl residue (Py) in the benzo[*a*]pyrene metabolite 7,8,9,10-tetrahydroxytetrahydrobenzo[*a*]pyrene (BPT) by the 2'-deoxynucleosides dG, dC, and dT in aqueous solutions. Time-correlated fluorescence single-photon counting techniques indicate that noncovalent [¹BPT–dN] complexes decay with lifetimes 200–300 faster than those of free singlet excited ¹BPT molecules. An unusual solvent kinetic isotope effect is observed: these lifetimes are longer by factors of 1.5–2.0 in D₂O than in H₂O. Nanosecond time scale transient absorption techniques show that BPT^{•+} radical cations are formed with yields $\phi_R = 0.07$ and 0.02 in 0.1 M aqueous dC and dT solutions, respectively, with similar yields of ³BPT triplet excited states. In the case of dG, the products of the quenching reaction are BPT^{•-} radical anions ($\phi_R = 0.25$) and ³BPT ($\phi_T = 0.35$) in dimethyl sulfoxide (DMSO); in aqueous solutions, however, only ³BPT triplet excited states are observed on nanosecond time scales. This lack of ion radical products is accounted for in terms of a more rapid recombination of the intermediate [BPT^{•-}···dG^{•+}] radical–ion pair, which is facilitated by hydrophobic interactions in water. The striking difference in the directions of electron transfer from ¹BPT to the pyrimidines dC and dT on the one hand, and from the purine derivative dG to ¹BPT on the other, can be rationalized in terms of the redox potentials of the relevant donor–acceptor pairs. In the case of dC and dT, the thermodynamics of electron transfer are unfavorable unless coupled to a rapid proton transfer step; this effect accounts for the strong quenching in water and the kinetic solvent isotope effect, as well as for the observed lack of fluorescence quenching by dC and dT in the polar organic solvent DMSO.

1. Introduction

It is well established that physicochemical interactions between the DNA bases and polynuclear aromatic fluorophores strongly quench the fluorescence of the latter.^{1–8} Photoinduced

electron transfer appears to be the most likely mechanism of quenching since the redox potentials are of the appropriate magnitudes for polycyclic aromatic fluorophore–nucleic acid couples.^{9–15} However, photoinduced electron transfer mechanisms in complexes between polynuclear aromatic fluorophores and DNA, or the individual nucleic acid residues, have received relatively little attention. These mechanisms are of intrinsic interest because they take place in aqueous or partially aqueous environments, thus providing opportunities for studying the effects of hydrophobic interactions,^{16,17} hydrogen bonding,¹⁴ and proton transfer coupled to photoinduced electron transfer

* To whom correspondence should be addressed. Phone: (212) 998 8407. FAX: (212) 998 8421.

[†] On leave from the Institute of Chemical Physics at Chernogolovka, Russian Academy of Sciences, Chernogolovka 142432, Russia.

[⊗] Abstract published in *Advance ACS Abstracts*, April 15, 1995.

(1) (a) Geacintov, N. E.; Prusik, T.; Khosrofiyan, J. M. *J. Am. Chem. Soc.* **1976**, *98*, 6444. (b) Prusik, T.; Geacintov, N. E.; Tobiasz, C.; Ivanovic, V.; Weinstein, I. B. *Photochem. Photobiol.* **1979**, *29*, 223. (c) Hogan, M.; Dattagupta, N.; Whitlock, J. P., Jr. *J. Biol. Chem.* **1981**, *256*, 4504. (d) McLeod, M. C.; Mansfield, B. K.; Selkirk, J. K. *Carcinogenesis* **1982**, *3*, 1031. (e) Undeman, O.; Lycksell, P.-O.; Gräslund, A.; Astlind, T.; Ehrenberg, A.; Jernström, B.; Tjerneld, F.; Nordén, B. *Cancer Res.* **1983**, *43*, 1851. (f) Chen, F.-M. *J. Biomol. Struct. Dyn.* **1986**, *4*, 401. (g) Eriksson, M.; Eriksson, S.; Nordén, B.; Jernström, B.; Gräslund, A. *Biopolymers* **1990**, *29*, 1249. (h) Eriksson, M.; Kim, S. K.; Sen, S.; Gräslund, A.; Jernström, B.; Nordén, B. *J. Am. Chem. Soc.* **1993**, *115*, 1639.

(2) Tesler, J.; Cruickshank, K. A.; Morrison, L. E.; Netzel, T. L.; Chan, C. *J. Am. Chem. Soc.* **1989**, *111*, 7226.

(3) (a) Shahbaz, M.; Harvey, R. G.; Prakash, A. S.; Boal, T. R.; Zegar, I. S.; LeBreton, P. R. *Biochem. Biophys. Res. Commun.* **1983**, *112*, 1. (b) Abramovich, M.; Prakash, A. S.; Harvey, R. G.; Zegar, I. S.; LeBreton, P. R. *Chem.-Biol. Interact.* **1985**, *55*, 39. (c) Urano, S.; Price, H. L.; Fetzer, S. M.; Briedis, A. V.; Milliman, A.; LeBreton, P. R. *J. Am. Chem. Soc.* **1991**, *113*, 3881.

(4) Kelly, J. M.; van der Putten, W. J. M.; McConnell. *Photochem. Photobiol.* **1987**, *45*, 167.

(5) Dunn, D. A.; Lin, V. H.; Kochevar, I. E. *Photochem. Photobiol.* **1991**, *53*, 47.

(6) Atherton, S. J.; Harriman, A. *J. Am. Chem. Soc.* **1993**, *115*, 1816.

(7) Lianos, P.; Georghiou, S. *Photochem. Photobiol.* **1979**, *29*, 13.

(8) Van Houte, L. P. A.; Van Grondelle, R.; Retèl, J.; Westra, J. G.; Zinger, D.; Sutherland, J. C.; Kim, S. K.; Geacintov, N. E. *Photochem. Photobiol.* **1989**, *49*, 387.

(9) Löber, G.; Kittler, L. *Stud. Biophys.* **1978**, *73*, 25. (b) Kittler, L.; Löber, G.; Gollmoch, F. A.; Berg, H. *Bioelectrochem. Bioenerg.* **1980**, *7*, 503.

(10) Seidel, C. *Proc. SPIE: Biomol. Spectrosc. II* **1991**, *1432*, 91.

(11) (a) Margulis, L.; Pluzhnikov, P. F.; Mao, B.; Kuzmin, V. A.; Chang, Y. J.; Scott, T. M.; Geacintov, N. E. *Chem. Phys. Lett.* **1991**, *187*, 597. (b) Geacintov, N. E.; Mao, B.; France, L. L.; Zhao, R.; Chen, J.; Liu, T.-M.; Ya, N.-Q.; Margulis, L. A.; Sutherland, J. C. *Proc. SPIE: Time-Resolved Laser Spectrosc. Biochem. III* **1992**, *1640*, 774.

(12) Geacintov, N. E.; Zhao, R.; Kuzmin, V. A.; Kim, S. K.; Pecora, L. J. *Photochem. Photobiol.* **1993**, *58*, 185.

(13) Shafirovich, V. Ya.; Levin, P. P.; Kuzmin, V. A.; Thorgeirsson, T. E.; Kliger, D. S.; Geacintov, N. E. *J. Am. Chem. Soc.* **1994**, *116*, 63.

(14) O'Connor, D.; Shafirovich, V. Ya.; Geacintov, N. E. *J. Phys. Chem.* **1994**, *98*, 9831.

(15) Shafirovich, V. Ya.; Kuzmin, V. A.; Geacintov, N. E. *Chem. Phys. Lett.* **1994**, *22*, 185.

fluorescence quenching phenomena.^{6,18,19} Our interest is to evaluate the mechanisms of quenching associated with each of the four major bases in DNA and their derivatives. Using model systems, we have found that certain metabolite model compounds of benzo[a]pyrene with pyrene-like aromatic residues are ideal for such studies because both noncovalent complexes and covalently linked donor–acceptor couples are readily available.^{11–15}

Benzo[a]pyrene is metabolically transformed to the stereoisomeric diol epoxide²⁰ 7,8-dihydroxy-9,10-epoxy-7,8,9,10-tetrahydrobenzo[a]pyrene (BPDE) that binds noncovalently^{3,21} and covalently^{22,23} to purines and to purine bases in DNA. In aqueous solutions BPDE is unstable and its hydrolysis product 7,8,9,10-tetrahydroxytetrahydrobenzo[a]pyrene (BPT) has been used as a model compound to study the noncovalent interactions between benzo[a]pyrene metabolites and nucleic acids.^{12–14,21}

The fluorescence of pyrenyl residues in BPDE– or BPT–nucleic acid complexes is quite sensitive to their immediate microenvironment and is therefore a very useful tool for investigating their interactions with DNA and the conformational properties of the adducts.^{24,25} However, this fluorescence is strongly quenched.^{11–15} Interestingly, the efficiencies of quenching are not only temperature-²⁶ and solvent-dependent^{8,11,13,14} but also depend on the nature of the interacting nucleic acid bases.^{12,27} The fluorescence of pyrenyl residues (Py) is quenched by guanosine residues,^{11–14} 2'-deoxythymidine, 2'-deoxycytidine, and 2'-deoxyuridine.¹² However, 2'-deoxyinosine and 2'-deoxyadenosine residues in these complexes or adducts are at best very weak quenchers.^{12,27}

In this work, the origins of the fluorescence quenching mechanisms are explored in some detail employing time-correlated fluorescence single-photon counting and nanosecond

time scale transient absorption techniques. We have shown previously that the purine derivative 2'-deoxyguanosine (dG) and guanosine residues in covalent adducts act as electron donors while the Py residues are the electron acceptors, in either polar organic or aqueous media.^{13,14} Using the noncovalently interacting donor–acceptor pairs BPT and 2'-deoxynucleosides as model systems, we show here that the pyrimidine derivatives 2'-deoxythymidine (dT) and 2'-deoxycytidine (dC) are strong quenchers of the fluorescence of BPT in water, but are inactive in polar organic solvents such as DMSO. In aqueous media, the fluorescence quenching mechanism involves a photoinduced electron transfer mechanism that occurs in the opposite direction with the Py residues now acting as the electron donors. A remarkable solvent isotope effect is observed on the kinetics of the fluorescence decay of ¹BPT in H₂O and in D₂O. This kinetic isotope effect, as well as a consideration of the redox potentials of the electron donor–acceptor couples, suggests that the electron transfer is coupled with a proton transfer from water molecules to the corresponding radical anions of the pyrimidine bases. Taking the thermodynamics of the proton-coupled photoinduced electron transfer reactions into account, this mechanism can explain the lack of fluorescence quenching by pyrimidine derivatives in polar organic solvents, and their strong quenching activities in aqueous solutions.

2. Experimental Section

An AVIV Model 14DS UV–vis spectrophotometer (Aviv Associates, Lakewood, NJ) was used for measuring absorption spectra. Fluorescence emission spectra were measured with a Hitachi Model MPF-2A fluorescence spectrometer (Perkin-Elmer Corp., Norwalk, CT) which was interfaced with an IBM PS/2 computer for data collection and analysis.

Fluorescence decay profiles were recorded using a home-assembled time-correlated single-photon counting system based on a synchronously pumped dye laser running at 660 nm and cavity-dumped at 1.8 MHz. Emissive photons were collected at 90° with respect to the excitation beam (330 nm) and passed through a monochromator (400 nm). The detection system utilizes a Hamamatsu R2809U microchannel plate photomultiplier tube and a modified Tennelec constant fraction discriminator. Data analysis was made after deconvolution of the instrument response function (fwhm ≈ 60 ps).²⁸

Transient absorption spectra were recorded using a laser flash photolysis system based on a N₂ laser (Everett Research Laboratories) as an excitation source (337 nm, 10 ns pulse duration, 0.2 mJ/pulse, beam area ~8 × 1 mm). The transient absorbance was measured with an ILC Technology Illuminator, model PS 150-9, 100 W steady-state high-pressure xenon arc lamp with a superimposed high-voltage pulse (2 ms) to increase the intensity of light during the measurement. The kinetic decay curves were averaged over 200 laser pulses by a Tectronix TDS 620 digital oscilloscope coupled to an IBM PC computer.

The BPT was prepared by hydrolysis of racemic BPDE in aqueous solution.¹² The racemic *trans*-tetraols, used throughout this work, were separated from *cis*-tetraols by reversed-phase HPLC techniques.^{12,13} A Model L-6200 Intelligent Pump (Hitachi Instruments) was used for this purpose, employing a 10 × 250.0 mm Hypersyl-ODS column (Keystone Scientific) and a 55–65% linear gradient of methanol in 20 mM sodium phosphate buffer, pH 7, for 60 min (flow rate 3 mL/min, UV detection of product at 254 nm). Heavy water (99.9 atom % D) and spectrophotometric grade *N,N*-dimethylformamide (DMF), *N*-methylformamide (MF), formamide (FA), and dimethyl sulfoxide (DMSO) were from Aldrich, and were used without further purification. The nucleosides dG, dT, and dC were purified by G-10 Sephadex column chromatography as necessary (the necessity of removing impurities was assessed by comparing the efficiency of quenching of the fluorescence of BPT by highly purified and unpurified nucleosides).

(28) Chang, M. C.; Courtney, S. H.; Cross, A. J.; Gulotty, R. G.; Petrich, J. W.; Fleming, G. R. *Anal. Instrum.* **1985**, *14*, 433.

(16) (a) Tanford, C. *The Hydrophobic Effect*, 2nd ed; Wiley: New York, 1980. (b) Ben-Naim, A. *Hydrophobic Interactions*; Plenum: New York, 1980.

(17) Breslow, R. *Acc. Chem. Res.* **1991**, *24*, 159.

(18) Turró, C.; Chang, C. K.; Leroi, G. E.; Cukier, R. I.; Nocera, D. G. *J. Am. Chem. Soc.* **1992**, *114*, 4013.

(19) Cukier, R. I. *J. Phys. Chem.* **1994**, *98*, 2381.

(20) For reviews see, e.g.: (a) Conney, H. *Cancer Res.* **1982**, *42*, 4875.

(b) Singer, B.; Grunberger, D. *Molecular Biology of Mutagens and Carcinogens*; Plenum Press: New York, 1983. (c) Harvey, R. G. *Polycyclic Aromatic Hydrocarbons: Chemistry and Carcinogenicity*; Cambridge University Press: Cambridge, 1991.

(21) (a) Ibanez, V.; Geacintov, N. E.; Gagliano, A. G.; Brandimarte, S.; Harvey, R. G. *J. Am. Chem. Soc.* **1980**, *102*, 5661. (b) MacLeod, M. C.; Selkirk, J. K.; *Carcinogenesis* **1982**, *3*, 287. (c) MacLeod, M. C.; Smith, B.; McClay, J. J. *Biol. Chem.* **1987**, *262*, 1081. (c) Geacintov, N. E.; Brenner, H. C. *Photochem. Photobiol.* **1989**, *50*, 841.

(22) (a) Weinstein, I. B.; Jeffrey, A. M.; Jennette, K. W.; Blobstein, S. H.; Harvey, R. G.; Harris, C.; Autrup, H.; Kasai, H.; Nakanishi, K. *Science* **1976**, *193*, 592. (b) Koreeda, M.; Moore, P. D.; Wislocki, P. G.; Levin, W.; Conney, A. H.; Yagi, H.; Jerina, D. M. *Science* **1978**, *199*, 778.

(23) Cheng, S. C.; Hilton, B. D.; Roman, J. M.; Dipple, A. *Chem. Res. Toxicol.* **1988**, *2*, 334.

(24) (a) Jankowiak, R.; Lu, P.-Q.; Small, G. J. *Chem. Res. Toxicol.* **1990**, *3*, 39. (b) Jankowiak, R.; Small, G. J. *Anal. Chem.* **1989**, *61*, 1023A. (c) Marsch, G. A.; Jankowiak, R.; Suh, M.; Small, G. J. *Chem. Res. Toxicol.* **1994**, *7*, 98.

(25) (a) Zinger, D.; Geacintov, N. E.; Harvey, R. G. *Biochem. Biophys. Chem.* **1987**, *27*, 131. (b) Jernström, B.; Lycksell, P.-O.; Gräslund, A.; Nordén, B. *Carcinogenesis* **1984**, *5*, 1129. (c) Kim, S. K.; Brenner, H. C.; Soh, B. J.; Geacintov, N. E. *Photochem. Photobiol.* **1989**, *327*. (d) Geacintov, N. E.; Cosman, M.; Mao, B.; Alfano, A.; Ibanez, V.; Harvey, R. G. *Carcinogenesis* **1991**, *12*, 2099.

(26) (a) Ivanovic, V.; Geacintov, N. E.; Yamasaki, H.; Weinstein, I. B. *Biochemistry* **1978**, *17*, 1597. (b) Kim, S. K.; Geacintov, N. E.; Zinger, D.; Sutherland, J. C. In *Synchrotron Radiation in Structural Biology. Basic Life Sciences*; Sweet, R. M., Woodhead, A. D., Eds.; Plenum Press: New York, 1989; Vol. 51, p 187. (c) Zhao, R.; Liu, T.-M.; Kim, S.-K.; MacLeod, M. C.; Geacintov, N. E. *Carcinogenesis* **1992**, *13*, 1817.

(27) (a) Chen, J.; MacLeod, M. C.; Zhao, R.; Geacintov, N. E. *Carcinogenesis* **1993**, *14*, 1049. (b) Yamamoto, J.; Subramaniam, R.; Wolfe, A. R.; Meehan, T. *Biochemistry* **1990**, *29*, 3966.

Sample concentrations (pyrenyl chromophores) were 3–7 μM (absorption and fluorescence measurements) or 20–40 μM (transient absorption measurements). Time-resolved fluorescence studies were performed in air-equilibrated solutions. Before nanosecond transient absorption and steady-state fluorescence measurements, however, the cells were carefully flushed with argon to remove O_2 . All measurements were conducted at 23 ± 1 $^\circ\text{C}$.

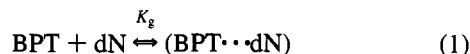
3. Results

The basic differences in the modes of quenching of the fluorescence of the Py residue of BPT by the nucleosides dG, dC, and dT can be demonstrated by studying the spectroscopic characteristics of these systems in polar organic and aqueous solvents.

3.1. Absorption and Fluorescence Characteristics in Aqueous and Polar Organic Solvents. The absorption and fluorescence quenching characteristics of BPT + dN solutions (dN = dG, dC, or dT) were compared in aqueous solutions and in DMSO; the latter medium was selected for study because of the high solubilities of the nucleosides in this polar organic solvent.

In DMSO, the absorption spectra of BPT remain unchanged as a function of nucleoside concentrations up to $[\text{dN}] \approx 1$ M. Therefore, the formation of noncovalent ($\text{BPT} \cdots \text{dN}$) ground state complexes in this and other polar organic solvents¹³ can probably be neglected.

In aqueous solutions, however, the addition of nucleosides results in pronounced shifts of the BPT absorption bands in the 320–360 nm region to longer wavelengths.^{12,13} The concentrations of dT and dC used in this work are much higher than those used previously.¹² Shifts in the absorption spectra of BPT in solution with the pyrimidine derivatives dC and dT are now clearly evident, especially at the higher concentrations (Figure 1). The spectral changes in solutions of BPT and nucleosides in D_2O are similar to those shown in Figure 1 (data not shown). Isobestic points in the absorption spectra are observed below concentrations of $[\text{dG}] < 0.02$ M and $[\text{dT}]$ and $[\text{dC}] < 0.07$ M, suggesting that 1:1 $\text{BPT} \cdots \text{dN}$ ground state complexes predominate at these low dN concentrations.^{12,13} However, at higher dN concentrations, the formation of complexes with a stoichiometry greater than 1:1 cannot be excluded because the isobestic points become more diffuse (data not shown). Thus, in aqueous solutions and in the lower concentration ranges, noncovalent 1:1 complexes predominate, as described by the following scheme:



where K_g is the ground state complex equilibrium association constant.

While the fluorescence emission spectra of BPT are not visibly perturbed by the nucleosides in DMSO, even at the highest concentrations, in aqueous solutions the 378 and 398 nm emission maxima are red-shifted by 1–2 nm and the vibronic bands are broadened by 5–6 nm (full width half-maximum); these effects are more pronounced at the highest dN concentrations and are attributed to the noncovalent singlet excited state $[\text{BPT} \cdots \text{dN}]$ complexes that are characterized by small but finite fluorescence yields.^{12,13}

Relative Fluorescence Yields in Polar Organic Solvents. In deoxygenated DMSO solutions the quenching of the fluorescence of BPT by the pyrimidine derivatives dC and dT is extremely weak even at the highest nucleoside concentrations of 1 M (Figure 2). In contrast, dG strongly quenches the fluorescence of BPT in this polar organic solvent; the Stern–

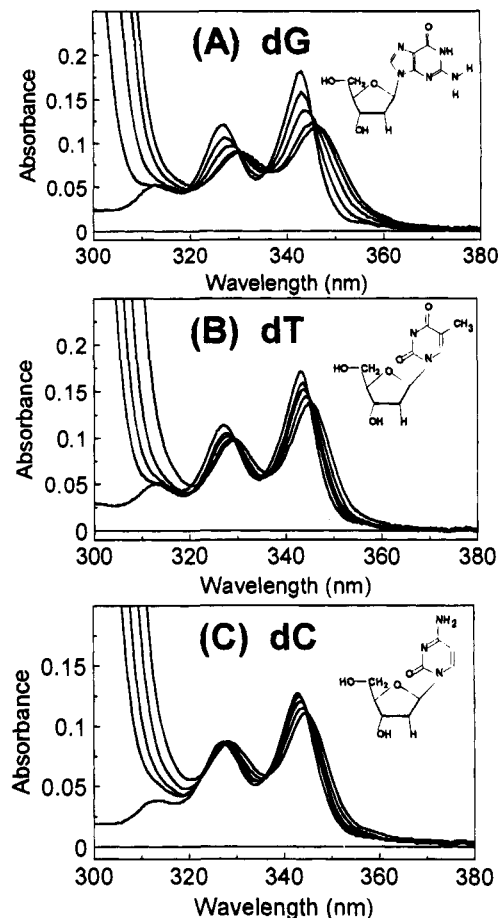


Figure 1. Absorption spectra of BPT in aqueous solutions at different concentrations of 2'-deoxynucleosides. The spectra with the highest absorbances at 343 nm are those of 2'-deoxynucleoside-free BPT solutions. These absorbances decrease as the concentrations of nucleosides are increased. The 2'-deoxynucleoside concentrations are (A) 0, 2.5, 7.5, 17.5, and 25 mM; (B) 0, 8, 16, 33, 67, and 100 mM; and (C) 0, 19, 38, 75, and 150 mM.

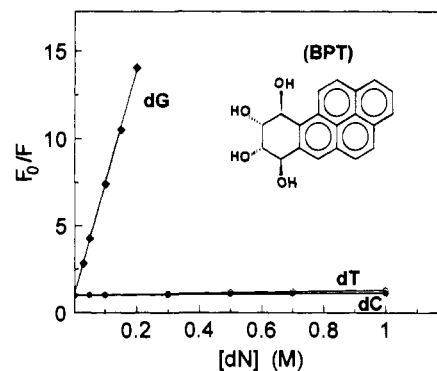


Figure 2. Stern–Volmer plots of the fluorescence yield ratio, F_0/F , as a function of the 2'-deoxynucleoside concentrations ($[\text{dN}]$) in deoxygenated DMSO solutions. The solid lines represent plots of the equation $F_0/F = 1 + (k_d/k_m)[\text{dN}]$ utilizing $k_d/k_m = 65$ M^{-1} (dG), 0.14 M^{-1} (dT), and 0.3 M^{-1} (dC), superimposed on the experimental data points. $[\text{BPT}] = 6.7$ μM .

Volmer plot is linear up to a dG concentration of at least 0.2 M. The bimolecular rate constant of fluorescence quenching, $k_d = (3.6 \pm 0.2) \times 10^8$ $\text{M}^{-1} \text{s}^{-1}$, can be calculated from the slope of the Stern–Volmer plot and the fluorescence decay time of ^1BPT , $\tau_0 = 180 \pm 10$ ns, in deoxygenated and nucleoside-free DMSO solutions. This value of k_d is only slightly lower than the value of $(4\text{--}7) \times 10^8$ $\text{M}^{-1} \text{s}^{-1}$ in solutions of amides¹³ (DMF, NMF, and FA).

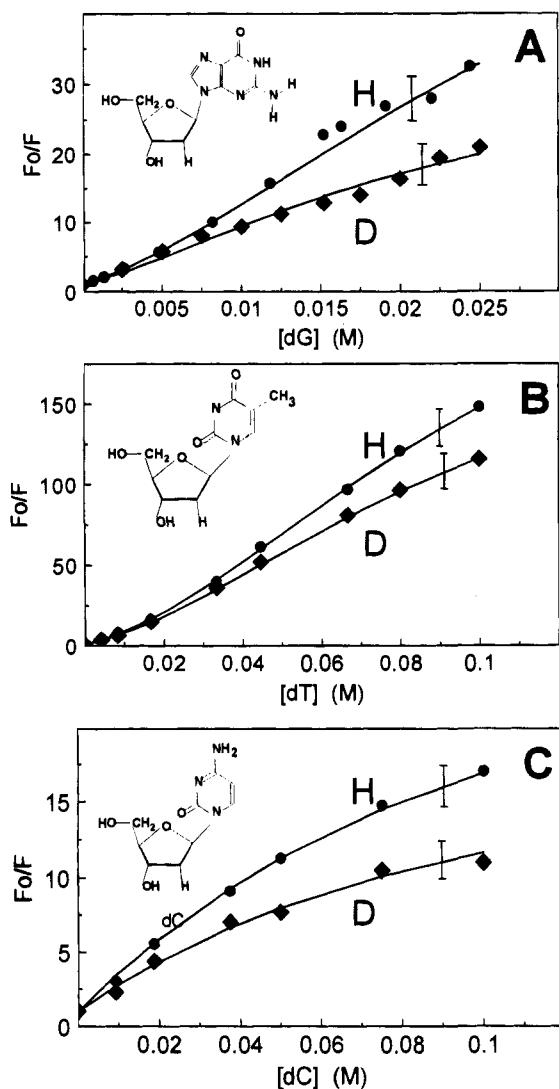


Figure 3. Stern-Volmer plots of the fluorescence yield ratio, F_0/F , as a function of 2'-deoxynucleoside concentrations in deoxygenated aqueous solutions: (●) in H_2O (H); (◆) in D_2O (D). The solid lines represent the best fits of eq 11 to the experimental data points with $k_m = 5 \times 10^6 \text{ s}^{-1}$, and the parameters (central values) given in Table 1; the vertical bars indicate the positions of these lines calculated with the error limits of the parameters indicated in Table 1. [BPT] = 6.7 μM .

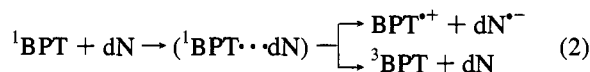
Relative Fluorescence Yields in Aqueous Solutions and the Deuterium Isotope Effect. In deoxygenated aqueous D_2O solutions, the relative fluorescence yield of BPT ($[dN] = 0$) is the same as in H_2O solutions. As in DMSO, dG is a quencher of the fluorescence of the BPT pyrenyl residue in H_2O and in D_2O , but the quenching efficiency is greater in the aqueous solutions (Figure 3A); in contrast to the lack of quenching observed in DMSO, in aqueous solutions the pyrimidine derivatives dC and dT are highly efficient quenchers of the fluorescence of BPT (Figure 3B,C). The integrated fluorescence yield values in the absence and presence of quenchers, F_0 and F , respectively, were measured using excitation at the isobestic point at 346 nm in order to avoid the trivial changes in the fluorescence signal levels related to variations in the absorption spectra (Figure 1). The Stern-Volmer F_0/F vs $[dN]$ plots deviate from linearity, particularly at the higher dN concentrations; these effects are attributed to the small, but finite, fluorescence yields of the noncovalent $[BPT \cdots dN]$ complexes (treated in detail below). In D_2O solutions, the F_0/F ratios are

lower than in H_2O by factors of 1.3–1.5, particularly at the higher dN concentrations (Figure 3).

3.2. Transient Absorption Spectra: Evidence for Reverse Electron Transfer from Pyrenyl Singlets to Pyrimidine Bases in Aqueous Solutions. We first recall the absorption characteristic of the transient species that can arise from the photoexcitation of BPT.¹³ In deoxygenated DMSO solution, the 1BPT singlet excited states exhibit transient absorption maxima at $\lambda_{max} = 365$ and 490 nm; the triplet excited states 3BPT and radical anion $BPT^{\bullet-}$ are characterized by absorption maxima at 420 and 500 nm, respectively. The radical cation $BPT^{\bullet+}$ exhibits a transient absorption maximum at 455 nm. In the presence of dG (0.2 M in DMSO), the probability of 1BPT quenching, $\phi_q = k_d[dG]/(1/\tau_0 + k_d[dG])$, is close to unity ($\phi_q = 0.92$), as can be readily estimated from the values of $k_d = (3.6 \pm 0.2) \times 10^8 \text{ M}^{-1} \text{ s}^{-1}$ and $\tau_0 = 180 \pm 10 \text{ ns}$, as noted above. Just as in the amide solvent DMF,¹³ the products of nanosecond laser pulse excitation of the BPT chromophore in the presence of dG in DMSO give rise to 3BPT and $BPT^{\bullet-}$ radical anion products (data not shown) with quantum yields of $\phi_T = 0.35$ and $\phi_R = 0.25$, respectively. In DMSO as well as in amides, the pyrimidine derivatives dC and dT do not quench the fluorescence of BPT and, consistent with this fact, radical ion products are not observed either.

In deoxygenated aqueous solutions, the bases dG, dC, and dT strongly quench the fluorescence of 1BPT , and the corresponding k_d values are shown in Table 1. In the presence of $[dG] = 0.025 \text{ M}$, corresponding to efficient quenching of 1BPT ($\phi_q = 1 - F/F_0 = 0.97$), the major transient product of the quenching reaction detectable in the nanosecond region is the triplet excited state 3BPT ($\phi_T = 0.09$) (Figure 4); radical ions are not observed ($\phi_R < 0.01$). The observed yield of 3BPT is a factor of 6 greater than the yield expected from the normal intersystem crossing mechanism that can be calculated from the formula $\phi_T = \phi_{T_0} F/F_0 \approx 0.5 \times 0.03 = 0.015$.¹³

In contrast to the lack of quenching in DMSO, in 0.1 M aqueous solutions of dC and dT, the quenching of the fluorescence is very efficient ($\phi_q = 0.94$ and 0.99, respectively); the transient absorption spectra exhibit maxima at 420 nm due to triplet excited states ($\phi_T = 0.06$ and 0.02, respectively). As in the case of dG,^{13,15} we observed that the yields of 3BPT are greater by factors of 2 and 7 than those predicted by the equation $\phi_T = \phi_{T_0} F/F_0$, for dC and dT, respectively. In addition to the triplet-triplet absorption maximum at 420 nm, prominent absorption maxima are also observed at 455 nm (Figure 4); these latter bands are attributed to $BPT^{\bullet+}$ radical cations, and their quantum yields are $\phi_R = 0.07$ and 0.02 in 0.1 M dC and dT solutions, respectively. The absence of hydrated electrons with a broad maximum around 700 nm²⁹ indicates that the direct photoionization of BPT, which is very efficient in aqueous solutions,¹³ is not responsible for the formation of $BPT^{\bullet+}$ under our experimental conditions; furthermore, if a BPT solution of the same concentration, but in the absence of dC or dT, is irradiated with 355 nm laser pulses under the same conditions, $BPT^{\bullet+}$ radical cations are not observed. Thus, we conclude that, in aqueous solutions, quenching of 1BPT by the pyrimidine bases result in formation of $BPT^{\bullet+}$ radical cations and 3BPT triplets. These events can be summarized as follows:



where dN is dC or dT. According to this scheme, radical anions $dC^{\bullet-}$ and $dT^{\bullet-}$ or their protonated forms $dC(H)^{\bullet}$ and $dT(H)^{\bullet}$

Table 1. Parameters of Dynamic and Static Fluorescence Quenching in Aqueous Solutions of Noncovalent BPT–Nucleoside Systems

parameter	BPT–dG		BPT–dT		BPT–dC	
	H ₂ O	D ₂ O	H ₂ O	D ₂ O	H ₂ O	D ₂ O
K_s^a (M ⁻¹)	180 ± 50	180 ± 50	60 ± 20	60 ± 20	10 ± 5	10 ± 5
K_e^b (M ⁻¹)	600 ± 200	600 ± 200	100 ± 30	100 ± 30	40 ± 15	40 ± 15
k_d (10 ⁹ M ⁻¹ s ⁻¹)	3.0 ± 0.3	2.5 ± 0.3	2.9 ± 0.3	2.5 ± 0.3	1.4 ± 0.2	1.0 ± 0.2
k_{-d} (10 ⁷ s ⁻¹)	0.5 ± 0.2	0.4 ± 0.2	3.0 ± 1.0	2.5 ± 0.3	3.5 ± 1.0	3.0 ± 1.0
k_c (10 ⁸ s ⁻¹)	1.9 ± 0.2	0.9 ± 0.1	17 ± 2	12 ± 1	1.8 ± 0.2	1.3 ± 0.1
ϕ	0.3 ± 0.1	0.3 ± 0.1	0.7 ± 0.3	0.7 ± 0.3	0.5 ± 0.2	0.5 ± 0.2

^a K_e calculated from values of k_d and k_{-d} (see text). ^b Calculated from the data in Figure 1 using methods described in refs 12 and 13.

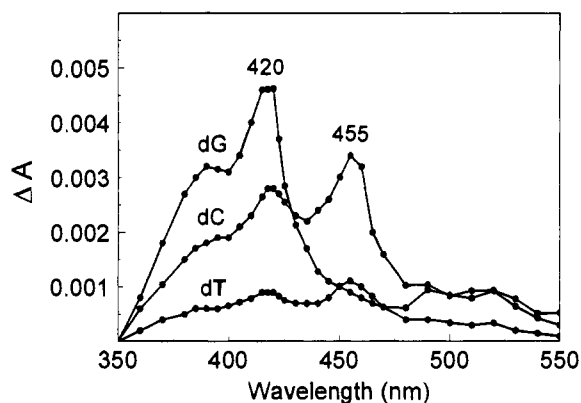


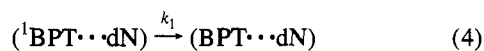
Figure 4. Transient absorption spectra of BPT–dN deoxygenated aqueous solutions: (1) [dG] = 20 mM; (2) [dC] = 100 mM; (3) [dT] = 100 mM. $\lambda(\text{excitation}) = 337$ nm, ~ 2.5 mJ/cm²/pulse, measured with a delay time $\Delta t = 10$ ns after the excitation laser flash. [BPT] = 30 μ M.

should also be generated, but were not detected in our transient absorption spectra; this is most likely due to their relatively small extinction coefficients³⁰ over a wide range of wavelengths ($\epsilon < 5 \times 10^3$ M⁻¹ cm⁻¹ from 350 to 550 nm).

3.3. Time-Resolved Fluorescence Characteristics in Aqueous Solutions. Kinetic Deuterium Isotope Effect. In air-equilibrated aqueous solutions, the fluorescence lifetimes of BPT (within experimental error, $\tau_0 = 135 \pm 10$ ns in both H₂O and D₂O) are somewhat less than those in deoxygenated aqueous solutions¹³ ($\tau_0 = 200 \pm 10$ ns), due to quenching by molecular oxygen. In the presence of dG or the two pyrimidine derivatives dC and dT, the fluorescence lifetimes of BPT pyrenyl residues are significantly shortened. A typical fluorescence decay profile of BPT in a 15 mM dG solution in H₂O is shown in Figure 5. The observed fluorescence decay profiles can be analyzed in terms of two exponential decay terms with a “fast” component and a “slow” component with lifetimes of τ_1 and τ_2 , and relative amplitudes A_1 and A_2 , respectively (with $A_1 + A_2 = 1$):

$$I_f(t) = A_1 \exp(-t/\tau_1) + A_2 \exp(-t/\tau_2) \quad (3)$$

The relative amplitude of the fast component (A_1) increases with increasing concentrations of nucleosides (Figure 6), whereas the corresponding rate constant $k_1 = 1/\tau_1$ exhibits, at best, a very weak dependence on the nucleoside concentration (Figure 7). This behavior is consistent with the notion that the fast decay component is due to the weak fluorescence of [BPT···dN] ground state complexes (static quenching):



The values of k_1 are arranged in the order $k_1(\text{dG}) \approx k_1(\text{dC}) <$

(30) Visscher, K. J.; Spoelder, H. J. W.; Loman, H.; Hummel, A.; Hom, M. L. *J. Radiat. Biol.* **1988**, *54*, 787.

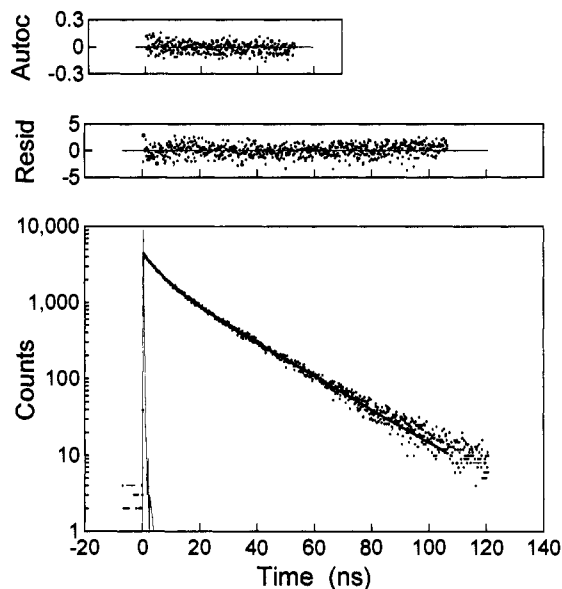
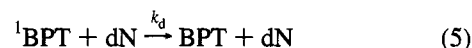


Figure 5. Fluorescence decay profiles of BPT (6.7 μ M) in air-equilibrated aqueous solutions of dG (15 mM). The solid line represents the best fit of a two-exponential function (eq 3) superimposed on the experimental data points, using the parameters $A_1 = 0.504$, $\tau_1 = 5$ ns, $A_2 = 0.496$, $\tau_2 = 19.7$ ns, and $\chi^2 = 1.2$; the residuals and autocorrelation function showing the goodness of fit are also depicted.

$k_1(\text{dT})$. Again, there is a solvent isotope effect: in D₂O solutions the values of k_1 are lower than in H₂O solutions by factors of 1.5–2.

The relative amplitude of the slow component (A_2) decreases and the corresponding rate constant $k_2 = 1/\tau_2$ increases with increasing concentrations of nucleosides (Figures 6 and 7). The slow component is due to the dynamic fluorescence quenching process:



The bimolecular quenching constant (k_d) can be estimated from the initial slopes of the k_2 vs [dN] plots, and these values are summarized in Table 1. In aqueous solutions, the quenching constants k_d for dG and dT are similar to one another in value ($k_d = (2.5\text{--}3.0) \times 10^9$ M⁻¹ s⁻¹), and are larger than the corresponding value for dC by a factor of about 2. These values of k_d are very close to the rate constants measured previously in a lower concentration range of dN.¹² Interestingly, in D₂O the values of k_d are lower than in H₂O solutions by factors of 1.1–1.4.

4. Discussion

We first discuss the opposite directions of photoinduced electron transfer in the case of dG on the one hand, and dC and dT on the other. Then the evidence for a proton-coupled electron transfer mechanism is reviewed, and we finally analyze

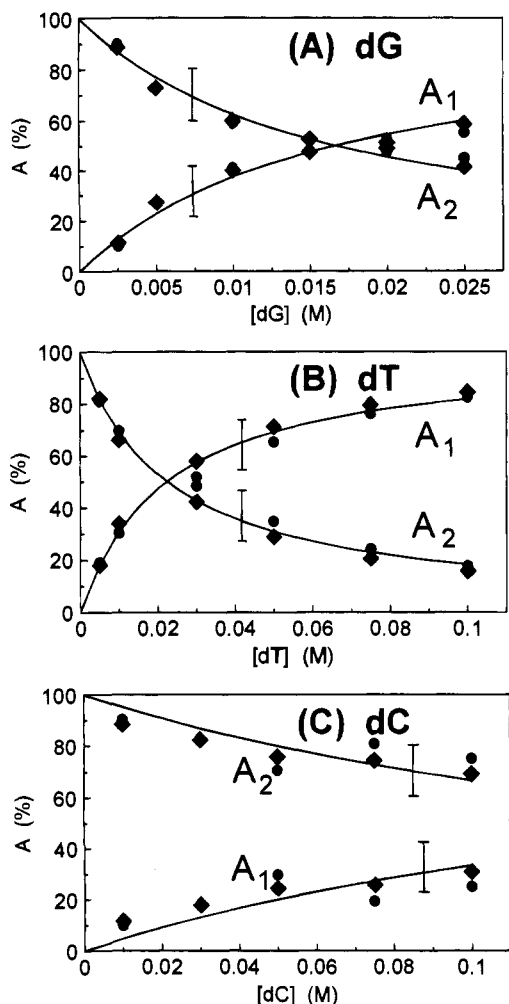


Figure 6. Dependence of the relative amplitudes A_1 and A_2 on the 2'-deoxynucleoside concentrations in air-equilibrated aqueous solutions: (●) in H_2O ; (◆) in D_2O . The solid lines represent the best fits to the experimental data points of the relative amplitudes calculated from eqs S4 and S5, utilizing $k_m = 7.4 \times 10^6 \text{ s}^{-1}$, the values of λ_1 and λ_2 determined from eq 10, and the parameters (central values) given in Table 1; the vertical bars indicate the positions of these lines calculated with the error limits of the parameters indicated in Table 1. [BPT] = $6.7 \mu\text{M}$.

quantitatively the effects of [$^1\text{BPT} \cdot \text{dN}$] complex formation and fluorescence quenching in H_2O and D_2O solutions.

The Directions of Photoinduced Electron Transfer Depend on the Nature of the Nucleosides. The following observations can be rationalized by considering the redox characteristics of the nucleic acid bases: (1) the lack of quenching of the BPT fluorescence by dC and dT in polar organic solvents, (2) their strong quenching efficiencies in aqueous solutions, (3) the opposite directions of electron transfer in which the purine quencher dG is an electron donor, while the pyrimidine derivatives dC and dT are electron acceptors, and (4) the solvent deuterium isotope effect.

The thermodynamic driving force, ΔG° , for the photoinduced electron transfer between the ^1BPT singlets and nucleosides can be estimated from the Rehm–Weller equation.³¹ For reductive quenching of the pyrenyl residue in ^1BPT , this equation can be expressed as follows:

$$\Delta G^\circ = e[E^\circ(\text{dN}^{\bullet+}/\text{dN}) - E^\circ(\text{Py}/\text{Py}^{\bullet-})] - \Delta E_{00} + w \quad (6)$$

(31) Rehm, D.; Weller, A. *Isr. J. Chem.* **1970**, *8*, 259.

The redox potential of the aromatic pyrenyl ring system in ^1BPT should not be too different from the redox potential of pyrene³² itself, $E^\circ(\text{Py}/\text{Py}^{\bullet-}) = -2.09 \text{ V}$ vs SCE³³ in DMF. The singlet excited state energy³⁴ of ^1BPT is $\Delta E_{00} = 3.28 \text{ eV}$. For quenching via the encounter complex with formation of the corresponding solvent-separated radical ion pair, the Coulombic energy term w is negligible in polar media³⁵ ($|w| < 0.1 \text{ eV}$). Hence, the reductive electron transfer from dN to ^1BPT is thermodynamically favored as long as $E^\circ(\text{dN}^{\bullet+}/\text{dN}) < 1.19 \text{ V}$ vs SCE. Unfortunately, the redox potentials of nucleosides are not well established since the nucleic acid bases exhibit irreversible oxidation in aqueous⁹ and aprotic media.¹⁰ On the basis of extensive studies of the interactions of ionizing radiation with DNA, it has been shown that the guanine residue is the most easily oxidized base in DNA.³⁶ This is consistent with the fact that, among the four most common DNA bases, dG exhibits the lowest gas phase ionization potential:³⁷ 8.0 (dG), 8.4 (dA), 8.6 (dC), and 8.7 eV (dT). Lecomte et al.,³⁸ on the basis of the data of Kittler et al.,⁹ have provided the following estimates of potentials for the irreversible oxidation of 2'-deoxynucleotide-5'-monophosphates in aqueous solutions: $E_{\text{ox}}(\text{GMP}^{\bullet+}/\text{GMP}) = 1.29 < E(\text{TMP}^{\bullet+}/\text{TMP}) = 1.49 < E(\text{CMP}^{\bullet+}/\text{CMP}) = 1.64 \text{ V}$ vs SCE. In aqueous solutions at pH 13 when nucleosides exist in their deprotonated forms, the same relative trend of redox potentials was obtained from electron transfer equilibria involving $\text{dN}(-\text{H})^\bullet$ species produced by pulse radiolysis and by reference to molecules with known redox potentials:³⁹ $E^\circ[\text{dG}(-\text{H})^\bullet/\text{dG}(-\text{H})^-] = 0.47 \text{ V} < E^\circ[\text{dT}(-\text{H})^\bullet/\text{dT}(-\text{H})^-] = 0.55 < E^\circ[\text{dC}(-\text{H})^\bullet/\text{dC}(-\text{H})^-] = 0.57 \text{ V}$ vs SCE. From $E^\circ[\text{dG}(-\text{H})^\bullet/\text{dG}(-\text{H})^-] = 0.47 \text{ V}$ vs SCE and the corresponding $\text{p}K_a$ values⁴⁰ for dG ($\text{p}K_a = 9.4$) and $\text{dG}(-\text{H})^\bullet$ ($\text{p}K_a = 3.9$), a value of $E^\circ(\text{dG}^{\bullet+}/\text{dG}) = 0.79 \text{ V}$ vs SCE in H_2O can be estimated.¹³ This estimate of $E^\circ(\text{dG}^{\bullet+}/\text{dG})$ indicates that electron transfer from dG to ^1BPT is thermodynamically favored since $\Delta G^\circ = -0.4 \text{ eV}$; indeed, the formation of BPT radical anions is observed in solutions of dG, at least in strong polar organic solvents.^{13,14}

In contrast to the results in polar organic solvents,¹³ in aqueous solutions $\text{BPT}^{\bullet-}$ radical anions are not observed. This suggests that the radical–ion pairs recombine more rapidly in aqueous solutions than in polar organic solvents and thus do not escape into the bulk solvent. A possible cause of this phenomenon is the hydrophobic effect,^{16,17} which can be defined as the tendency of nonpolar molecules (e.g., the aromatic ring systems of the two interacting moieties) to aggregate in water, thus decreasing the solute–water contacts. The hydrophobic

(32) Kubota, T.; Kano, J.; Uno, B.; Konse, T. *Bull. Chem. Soc. Jpn.* **1987**, *60*, 3865.

(33) In this work all E values are defined relative to the saturated calomel electrode (SCE). In some references, the values of E are stated relative to NHE (normal hydrogen electrode); these values were converted into E vs SCE values by subtracting 0.24 V from the E vs NHE values.

(34) The observed vibronic BPT transitions with a maximum at 345 nm are due to the $S_2 \leftarrow S_0$ transition, while the $S_1 \leftarrow S_0$ transition threshold of BPT occurs near 378 nm, and thus $\Delta E_{00} = 3.28 \text{ eV}$.

(35) Bolton, J. R.; Archer, M. D. In *Electron Transfer in Inorganic, Organic, and Biological Systems*; Bolton, J. R., Mataga, N., McLendon, G., Eds.; Advances in Chemistry Series 228; CSC Symposium Series 2; The American Chemical Society: Washington, DC, 1991; p 7.

(36) (a) Al-Kazwini, A. T.; O'Neil, P.; Fielden, E. M.; Adams, G. E. *Radiat. Phys. Chem.* **1988**, *32*, 385. (b) Al-Kazwini, A. T.; O'Neil, P.; Adams, G. E.; Fielden, E. M. *Radiat. Res.* **1990**, *121*, 149. (c) Yan, M.; Becker, D.; Summerfield, S.; Renke, P.; Seliva, M. D. *J. Phys. Chem.* **1992**, *96*, 1983. (d) Candeias, L. P.; Jones, G. D. D.; O'Neil, P.; Steenken, S. *Int. J. Radiat. Biol.* **1992**, *61*, 15. (e) Candeias, L. P.; Steenken, S. *J. Am. Chem. Soc.* **1993**, *115*, 2437.

(37) Hush, N. S.; Cheung, A. S. *Chem. Phys. Lett.* **1975**, *34*, 11.

(38) Lecomte, J.-P.; Kirsh-De Mesmaeker, A.; Kelly, J. M.; Tossy, A. B.; Görner, H. *Photochem. Photobiol.* **1992**, *55*, 681.

(39) Jovanovich, S. V.; Simic, M. G. *J. Phys. Chem.* **1986**, *90*, 974.

(40) Candeias, L. P.; Steenken, S. *J. Am. Chem. Soc.* **1989**, *111*, 1094.

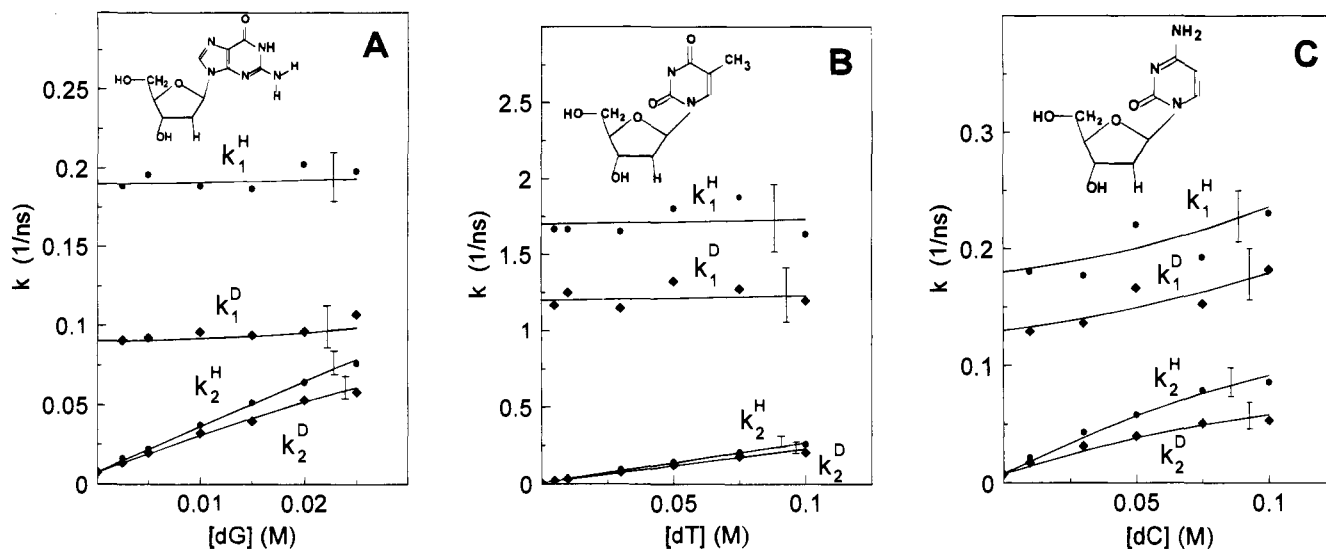


Figure 7. Dependence of the rate constants $k_1^{H,D}$ and $k_2^{H,D}$ (where superscripts H and D are related to H₂O and D₂O solutions) on the 2'-deoxynucleoside concentrations in air-equilibrated aqueous solutions. The solid lines represent the best fits of eq 10 ($\lambda_1 = k_1$ and $\lambda_2 = k_2$) to the experimental data points utilizing $k_m = 7.4 \times 10^6 \text{ s}^{-1}$ and the parameters (central values) given in Table 1; the vertical bars indicate the positions of these lines calculated with the error limits of the parameters indicated in Table 1. [BPT] = 6.7 μM .

effect thus tends to prevent the escape of BPT^{•-} and dG^{•+} into the bulk of the aqueous solution, ion pair recombination occurs, and ³BPT is the only observable product of the fluorescence quenching reaction. The mechanism of triplet formation with yields significantly greater than those expected from a normal intersystem crossing mechanism^{13,15} is believed to occur via this type of recombination mechanism as discussed in the case of other intermediate radical pair ions.^{41,42} An important requirement for the observation of an enhanced triplet yield is that the energy of the radical-ion pair must be greater than the energy of the triplet state; since the energy of ³BPT⁴³ ($E_{0,0} = 2.1 \text{ eV}$) is lower than that of the radical pairs (energy $E \approx 2.9 \text{ eV}$), this requirement is satisfied.

In agreement with the relative abilities of electron abstraction from nucleotides, Lecomte et al.³⁸ found that in aqueous solutions the electron transfer rates from nucleotides to the excited state of ruthenium tris(1,4,5,8-tetraazaphenanthrene) exhibit the order 2.2×10^{10} (GMP), $< 3 \times 10^8$ (dAMP) $< 1 \times 10^8$ (CMP), and $< 1 \times 10^8$ (TMP). Since GMP is ~ 100 times more efficient as a quencher than the other three nucleotides, it is not surprising that adenosine and the pyrimidine bases do not quench the fluorescence of ¹BPT by an analogous reductive electron transfer mechanism.

For oxidative electron transfer quenching of Py residues, with the bases dN acting as the electron acceptors, the Rehm-Weller equation³¹ can be expressed as follows:

$$\Delta G^\circ = e[E^\circ(\text{Py}^{•+}/\text{Py}) - E^\circ(\text{dN}/\text{dN}^{•-})] - \Delta E_{0,0} + w \quad (7)$$

The redox potential of the pyrenyl residue in BPT should not be too different from the redox potential of pyrene, $E^\circ(\text{Py}^{•+}/\text{Py}) = 1.28 \text{ V vs SCE}$ in DMF.³² The oxidative electron transfer from ¹BPT to dN is thermodynamically favored as long as $E^\circ(\text{dN}/\text{dN}^{•-}) > -2.0 \text{ V vs SCE}$. The electron affinities of nucleic acid bases, derived from MO calculations, show that

(41) (a) Orbach, N.; Ottolenghi, M. *Chem. Phys. Lett.* **1975**, *35*, 175. (b) Orbach, N.; Ottolenghi, M. In *The Exciplex*; Gordon, M., Ware, W. R., Eds.; Academic Press: New York, 1975; p 75.

(42) (a) Schulten, K.; Staerk, H.; Weller, A.; Werner, H.-J.; Nickel, B. *Z. Phys. Chem. N. F.* **1976**, *101*, 371. (b) Weller, A.; Staerk, H.; Treichel, R. *Faraday Discuss. Chem. Soc.* **1984**, *78*, 271.

(43) Kolubaev, V.; Brenner, H. C.; Geacintov, N. E. *Biochemistry* **1987**, *26*, 2638.

the purines are less electron-affinic than the pyrimidines.⁴⁴ Consistent with this conclusion, EPR studies⁴⁵ have shown that the pyrimidine bases dT and dC in DNA nucleotides are the most effective traps of negative charges produced by ionizing radiation,⁴⁶ and that purine electron adducts readily transfer their excess negative charge to pyrimidines.⁴⁷ Quantitative estimates of the electrochemical reduction potentials of nucleosides are difficult to obtain because redox reactions are irreversible even in aprotic media such as DMF and DMSO; therefore, only crude estimates of the dN redox potentials are available:^{10,48} $E^\circ(\text{dG}/\text{dG}^{•-}) < -2.7$, $E^\circ(\text{dC}/\text{dC}^{•-}) = -2.5$, and $E^\circ(\text{dT}/\text{dT}^{•-}) = -2.4 \text{ V vs SCE}$. However, even these crude estimates show that the energy of the radical pair is greater than the energy of the BPT singlet excited state and hence the oxidative electron transfer from ¹BPT to dN is thermodynamically unfavorable, at least in strong polar aprotic media (the energy level scheme for the BPT/dC system is summarized in Scheme 1, with the numbers designating the energies). In agreement with these considerations we have not found any evidence for the oxidative quenching pathway in strong polar amides and in DMSO.

Proton-Coupling Affects the ΔG° Values of Photoinduced Electron Transfer from ¹BPT to Pyrimidine Derivatives. In aqueous solutions, protonation of the electron adducts of pyrimidine derivatives is a rapid process^{48,49a} that can significantly affect the redox properties of nucleosides in aqueous solutions.⁴⁹ Conventional electrochemical measurements have shown that reduction potentials of nucleosides shift positively due to the protonation of the reduced species.⁵⁰ Conductivity measurements^{48,49a} have shown that the electron adducts of cytosine residues are protonated at N(3) in aqueous solutions at pH 6–10.5. Protonation of these electron adducts is complete

(44) (a) Pullman, B.; Pullman, A. *Quantum Biochemistry*; Wiley-Interscience: London, 1963. (b) Berthod, H.; Giessner-Pretre, C.; Pullman, A. *Theor. Chim. Acta* **1966**, *5*, 53. (c) Bodor, N.; Dewar, M. J. S.; Harget, A. J. *J. Am. Chem. Soc.* **1970**, *92*, 2929. (d) Compton, R. N.; Yoshioka, Y.; Jordan, K. D. *Theor. Chim. Acta* **1980**, *54*, 259. (e) Ravkin, B.; Herak, J. N. *Radiat. Phys. Chem.* **1983**, *22*, 1043.

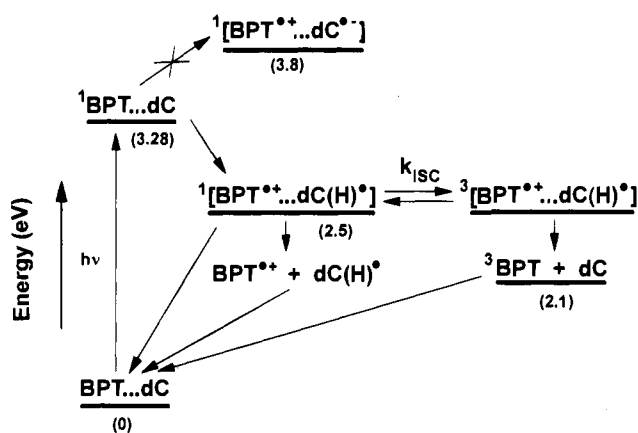
(45) (a) Gregoli, S.; Olast, M.; Bertinchamps, A. *Radiat. Res.* **1977**, *70*, 255. (b) Gregoli, S.; Olast, M.; Bertinchamps, A. *Radiat. Res.* **1979**, *77*, 417. (c) Gregoli, S.; Olast, M.; Bertinchamps, A. *Radiat. Res.* **1982**, *89*, 238.

(46) For reviews see: (a) Von Sonntag, C.; Schuchmann, H.-P. *Int. Radiat. Biol.* **1986**, *49*, 1. (b) Steenken, S. *Chem. Rev.* **1989**, *89*, 503.

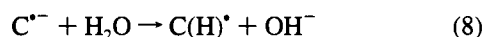
(47) Cummings, T. E.; Elving, P. J. *J. Electroanal. Chem.* **1978**, *4*, 123.

(48) Hissung, A.; Sonntag, C. *Int. J. Radiat. Biol.* **1979**, *35*, 449.

Scheme 1

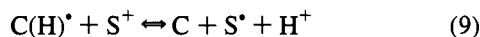


within ≤ 10 – 20 ns, and water acts as an acid in this reaction:



A lower limit of the $\text{p}K_a$ (≥ 13) for the protonated electron adduct has been estimated.^{30,48}

The redox potential $E(\text{dC}/\text{dC}(\text{H})^{\bullet})$ can be estimated from data provided for other cytosine derivatives since the deoxyribose residue is not expected to affect the redox potentials.^{49a} The hydrated electron adducts of cytidine ($\text{C}(\text{H})^{\bullet}$) undergo reversible electron transfer with pyrimidinium ion standards (S^+) of known reduction potentials as follows:^{49a}



and reduction potentials of $E(\text{dC}/\text{dC}(\text{H})^{\bullet}) = -1.33$ V vs SCE can be estimated from the data provided by Steenken et al.^{49a} vs NHE reference electrodes³³ (here we recalculated all potentials by subtracting 0.24 V from the NHE values to obtain the SCE values). Thus, protonation of the electron adducts provides an additional driving force to the overall reduction of cytosine derivatives, and the reduction potential becomes more positive than in the absence of protonation. The energetics of these processes are summarized in Scheme 1; according to this scheme, oxidative photoinduced electron transfer from ^1BPT to dC is thermodynamically not favored, unless accompanied by proton transfer from water to the pyrimidine radical anions. Again using pyridinium cation standards of known reduction potentials, the redox potentials of a number of thymine derivatives have been determined and are equal to $E = -1.33$ V vs SCE in aqueous solutions.^{49a} The dramatic difference in

(49) (a) Steenken, S.; Telo, J. P.; Novais, H. M.; Candeias, L. P. *J. Am. Chem. Soc.* **1992**, *114*, 4701. (b) We note here that the measured value $E(\text{dT}/\text{dT}^{\bullet-})$ of -1.33 vs SCE (or -1.09 vs NHE) provided by Steenken et al.^{49a} is difficult to rationalize without assuming that a proton transfer step is coupled to the electron transfer reaction on the nanosecond or subnanosecond time scales, as is the case for the reduction of dC in aqueous solutions^{49a} (eq 8). Values^{10,47} of $E(\text{dC}/\text{dC}^{\bullet-}) = -2.5$ V and $E(\text{dT}/\text{dT}^{\bullet-}) = -2.4$ V vs SCE in DMF solution have been reported. In the case of dC, it is accepted that the reduction potential increases to -1.3 V vs SCE in aqueous solution due to a coupled proton transfer reaction.^{48,49a} A similar value is observed in the case of the reduction of dT in aqueous solution,^{49a} but Steenken et al. assigned this value to the simple reduction of dT ($E(\text{dT}/\text{dT}^{\bullet-}) = -1.33$ V vs SCE). However, it is reasonable to assume that this value pertains also to a proton-coupled electron transfer reaction with $E(\text{dT}/\text{dT}^{\bullet}) = -1.33$ V vs SCE. Otherwise, the differences in the $E(\text{dT}/\text{dT}^{\bullet-})$ values in DMF and in aqueous solutions of about $+0.9$ V are difficult to account for in terms of solvation effects without proton transfer. Our own fluorescence quenching data, coupled with the observed deuterium isotope effects, are consistent with the assignment of the value of -1.33 V vs SCE to the proton-coupled reduction of dT in aqueous solutions.

(50) (a) Janik, B.; Elving, P. J. *Chem. Rev.* **1968**, *68*, 295. (b) Elving, P. J.; Pace, S. J.; O'Reilly, J. E. *J. Am. Chem. Soc.* **1973**, *95*, 647.

the redox potentials of thymine derivatives in aqueous solutions ($E = -1.33$ V vs SCE^{49a}) and in aprotic polar organic solvents ($E = -2.4$ V vs SCE^{10,47}) cannot be easily attributed to effects of polarity or solvent–solute interactions; instead, this difference is most likely due to a fast protonation of the thymine radical anions by water, just as in the case of the cytosine residues.^{49b} The oxidative quenching of the pyrenyl fluorescence by pyrimidines thus becomes thermodynamically favorable in aqueous solutions because the coupled proton transfer step lowers the redox potential of the thymine residue from -2.4 to -1.33 V.

In this work we have found the first experimental evidence for the formation of $\text{BPT}^{\bullet+}$ radical cations in the quenching of ^1BPT by the pyrimidine bases dC and dT in aqueous solutions. This observation suggests that the escape of the radical ions into the bulk of the solution is consistent with the proton-coupled electron transfer mechanism; the attractive Coulomb potential that would hold the radical ion pair together is no longer existent if the pyrimidinyl anion is protonated. Nevertheless, the radical ion yields remain quite low, probably due to the hydrophobic effect^{16,17} that tends to reduce the probability of dissociation of the interacting species in aqueous solutions. The hydrophobic interactions between Py residues and pyrimidine moieties are in general weaker than with purine bases¹² (Table 1); this difference may account for the fact that radical ions are not observed in the dG quenching reactions in aqueous solutions, although such ions are readily observed in polar organic solvents.¹³

The formation of pyrenyl triplet excited states with yields significantly greater than those expected from a normal intersystem crossing mechanism is also consistent with the proton-coupled electron transfer mechanism (Scheme 1). The energy of the radical ion pair ($E \approx 2.5$ eV) for the oxidative quenching of ^1BPT by dT and dC is again greater than that of the triplet state, $^3\text{BPT}^{\bullet}$ ($E_{0,0} = 2.1$ eV), and triplet formation can occur via the intersystem crossing of the singlet radical ion pair to the triplet state with rate constant k_{ISC} (Scheme 1).

The major feature of the proton-coupled electron transfer from ^1BPT donors to the pyrimidine base acceptors is that the source of protons appears to be the solvent (water). The protonation by H^+ is not sufficiently rapid and is thus not likely to play a critical role in the nanosecond time scale quenching reactions observed in this as well as in earlier work.^{13,14} The participation of water in these quenching reactions is further supported by the lack of quenching of the ^1BPT fluorescence by dC and dT in DMSO (Figure 2). Therefore, the mechanism involving water as the proton donor is different from the hydrogen atom transfer reactions described previously in which both the electron and the proton are transferred between the donor–acceptor pairs.^{5,6,51,52} These processes include (1) the quenching of singlet excited states of pyrene by primary and secondary amines with free NH groups,⁵¹ (2) the fluorescence quenching of methylene blue by guanine residues in complexes with the synthetic polynucleotide poly[dG–dC],^{5,6} and (3) the photoinduced reactions of benzophenone with amines.⁵²

Deuterium Isotope Effect as Evidence of a Proton-Coupled Electron Transfer Mechanism. The participation of a proton transfer step in the photoinduced electron transfer quenching of the fluorescence of ^1BPT by nucleosides is supported by the solvent deuterium isotope effect. The deuterium isotope effect in proton-coupled electron transfer reactions can, in principle, influence one or more of the critical parameters of electron

(51) Okada, T.; Mori, T.; Mataga, N. *Bull. Chem. Soc. Jpn.* **1976**, *49*, 3398.

(52) Formosinho, S. J.; Arnaut, L. G. *Adv. Photochem.* **1991**, *16*, 67.

transfer,¹⁴ e.g., ΔG° , the electron exchange matrix element (V), and the reorganization energy (λ). For example, deuterium isotope effects on electron transfer rates in donor-acceptor systems hydrogen-bonded to one another have been explained in terms of the influence of deuteration on the matrix element V .^{18,19} In our case, the quenching of the fluorescence of ¹BPT by the pyrimidine derivatives dC and dT, the deuterium isotope effect is likely to be associated with differences in ΔG° as in other examples of hydrogen atom transfer reactions.^{51,52}

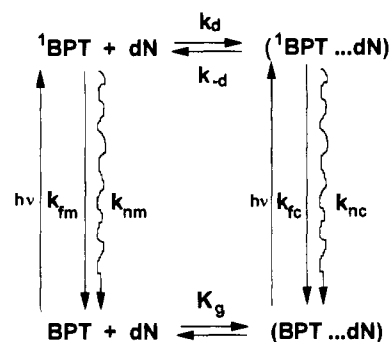
The fluorescence quenching of ¹BPT by dG also exhibits a deuterium isotope solvent effect (Figure 6), suggesting that here too an isotope-sensitive proton-coupled electron transfer step is operative. Since BPT^{•-} radical anions are observed in amide solvents,¹⁴ the guanine residue is the electron donor in polar organic solvents.¹³ In aqueous solutions, on the other hand, BPT^{•-} radical anions are not observed, presumably because of a more rapid ion pair recombination than in organic solvents, as discussed earlier.¹⁴ However, in the case of quenching by dG residues, the thermodynamics of oxidative electron transfer from ¹BPT are sufficiently favorable so that these processes can apparently occur even in polar organic solvents without the involvement of a proton-coupled step.

The deuterium isotope effects on the fluorescence decay rate constants and yields in BPDE-dG adducts¹⁴ and noncovalent BPT-dG complexes (Figure 7) may involve the release of a proton from the dG^{•+} radical cation since its $pK_a = 3.9$.⁴⁰ These differences could be due to isotope effects on ΔG° due to proton-coupling effects, or to isotope effects on the reorganization energies as discussed earlier.¹⁴

The overall differences in the fluorescence decay rate constants and yields in covalent BPDE-dG adducts¹⁴ and noncovalent BPT-dG systems (Figures 5 and 7) in aqueous solutions is noteworthy. The mean fluorescence decay times of the *cis*- and *trans*-BPDE-dG adducts¹⁴ are 0.67 and 1.4 ns, respectively, whereas in the noncovalent BPT-dG complexes the decay time is ~ 5 ns (Figure 5). In the latter case the 10 nm red shift in the absorption maxima and hypochromism (Figure 1A) suggests that base-pyrenyl residue stacking interactions are important in the noncovalent complexes. In the covalent BPDE-dG adduct the red shift is small (~ 2 nm) since the absorption maximum is at 345 nm,^{11a} and a parallel alignment of the pyrenyl moiety and guanine residue is not possible because of the bond angles in the covalent adduct. These results indicate that stacking interactions are not necessarily associated with an increased fluorescence quenching efficiency. Differences in spatial orientations of the donor-acceptor pair, as already noted for stereochemically different BPDE-dG covalent adducts,¹⁴ are of critical importance in determining the efficiency of quenching of the fluorescence of the pyrenyl residue.

Analysis of Fluorescence Quenching in Noncovalent BPT-Nucleoside Complexes in Aqueous Environments. The dependence of the fluorescence yield (Figure 3), the amplitudes of the two fluorescence components (Figure 6), and the decay constants k_1 and k_2 (Figure 7) can be accounted for in terms of Scheme 2 using solutions of the appropriate differential equations.⁵³ The terms k_{fm} , k_{fc} , k_{nm} , and k_{nc} denote the decay rate constants of free ¹BPT molecules (subscript m) and [¹BPT^{••}dN] excited state complexes (subscript c), the subscripts f and n denote fluorescence and nonradiative deactivation pathways, respectively, and k_d and k_{-d} are the rate constants for the formation and dissociation of the [¹BPT^{••}dN] complex, re-

Scheme 2



spectively. We define the equilibrium association constant as $K_e = k_d/k_{-d}$. The free molecular ¹BPT decay constant is $X = k_m + k_d[\text{dN}]$ with $k_m = k_{fm} + k_{nm}$. The value of $k_m = 1/\tau_0$ can be easily determined from the experimental fluorescence lifetime of free ¹BPT. The decay constant of the complexed ¹BPT molecules is $Y = k_c + k_{-d}$ with $k_c = k_{fc} + k_{nc}$.

The solution of standard differential equations⁵³ based on Scheme 2 yields expressions for the time dependence of the concentrations of free ¹BPT and [¹BPT^{••}dN] complexes and of the corresponding fluorescence intensities, following excitation with a δ -function light pulse at $t = 0$ (supplementary material, eqs S1-S3). The fluorescence decay can be described in terms of the usual sum of two exponentials (eq 3) with the eigenvalues:

$$\lambda_{1,2} = [X + Y \pm \{(Y - X)^2 + 4k_{-d}k_d[\text{dN}]\}^{1/2}]/2 \quad (10)$$

It is shown in the supplementary material that the relationships between the experimentally measured decay constants k_1 and k_2 and eq 10 are λ_1 (plus sign in eq 10) $\rightarrow k_1$ and λ_2 (minus sign) $\rightarrow k_2$. Furthermore, it is shown that all of the constant parameters in eq 10, except k_{-d} , can be estimated directly from the experimental data (Table 1). The values of k_{-d} can be obtained by finding the best fits of eq 10 to the experimental data in Figure 7 (solid lines), and are summarized in Table 1 as well. The values of k_c (Table 1) were obtained from the values of Y and k_{-d} .

For the photostationary state, the solution of the rate equations corresponding to Scheme 2 gives the following equation for the relative fluorescence yields:^{53b}

$$F_0/F = \frac{1 + k_d[\text{dN}]/k_m + k_{-d}/k_c}{\alpha + k_{-d}/k_c + (\phi k_m/k_c)(1 - \alpha + k_d[\text{dN}]/k_m)} \quad (11)$$

where $\alpha = 1/(1 + K_g[\text{dN}])$, and ϕ is equal to k_{fc}/k_{fm} , the ratio of radiative decay rate constants of free (k_{fm}) and complexed (k_{fc}) ¹BPT. In eq 11 all of the parameters defining the F_0/F ratio are known, except for ϕ . The values of ϕ can be estimated by fitting eq 11 to the experimentally measured F_0/F ratios using ϕ as a parameter. The calculated F_0/F ratios obtained in this manner are represented by the solid lines in Figure 3, and the corresponding values of ϕ are summarized in Table 1. The values of ϕ are less than unity. This indicates that the radiative rate constants of deactivation of the [¹BPT^{••}dN] complexes are lower than those for free ¹BPT ($k_{fm} > k_{fc}$).

Expressions for the dependences of the relative amplitudes A_1 and A_2 (eq 3) on the nucleoside concentrations are provided in the supplementary material (eqs S4 and S5). The amplitudes A_1 and A_2 are functions of the parameters given in Table 1, and represent the effective proportions of complexed and free ¹BPT molecules, respectively. The fits of eqs S4 and S5 to the

(53) (a) Birks, J. B. *Photophysics of Aromatic Molecules*; Wiley-Interscience: New York, 1970; Chapter 7. (b) Vaughan, W. M.; Weber, W. *Biochemistry* 1970, 9, 464. (c) Lakowicz, J. R. *Principles of Fluorescence Spectroscopy*; Plenum Press: New York, 1983.

experimentally determined amplitudes are represented by the solid lines in Figure 6.

The results in Table 1 indicate that, within experimental error, only the overall decay rate constant of the complexes, k_c , exhibits a deuterium isotope effect. In both H₂O and D₂O solutions, the values of k_d are lower by a factor of 2–5 than the values of the diffusion-controlled rate constant $k_{\text{dif}} = 6.5 \times 10^9$ (H₂O) and 5×10^9 (D₂O) M⁻¹ s⁻¹ calculated from the Smoluchowski equation:⁵⁴

$$k_{\text{dif}} = 8RT/3000\eta \quad (12)$$

where the viscosity⁵⁵ $\eta = 1.00$ cP in H₂O and 1.28 cP in D₂O. Although the calculation of the k_{dif} values using eq 12 is a very crude approximation for nonspherical molecules like BPT and dN, the fact that $k_d < k_{\text{dif}}$ is consistent with the notion that the quenching probability per collisional encounter, $p = k_d/k_{\text{dif}}$, is less than unity ($p \approx 0.2$ – 0.5).

The values of k_{-d} decrease in the order $dC \approx dT > dG$ (Table 1). This trend of the dissociation rate constants of the complexes indicates that the [¹BPT••dG] complexes are more stable than the ¹BPT–pyrimidine complexes.

The values of K_e for formation of the excited state complexes [¹BPT••dG] are greater than the corresponding values K_g for

the ground state complexes; this difference is attributed to the greater dipole moment of the ¹BPT excited state than that of the ground state,⁷ thus increasing the attractive interaction potential in the former. Both the K_e and K_g values have approximately similar values in H₂O and D₂O solutions, and decrease in the order $dG > dT > dC$.

Acknowledgment. This work was supported by Grant DE-FGO2-86ER06045 from the Office of Health and Environmental Research, U.S. Department of Energy. The laser fluorescence lifetime facility is supported by the National Science Foundation Instrumentation and Instrument Development Program, Award No. 9011268.

Supplementary Material Available: Text providing explicit solutions of differential equations⁵³ based on Scheme 2 for the time-dependent fluorescence due to free ¹BPT and [¹BPT••dN] following δ -pulse excitation, together with the calculated amplitudes A_1 and A_2 (cf. eq 3), and describing the methods for obtaining some of the constants in Table 1 in greater detail (3 pages). This material is contained in many libraries on microfiche, immediately follows this article in the microfilm version of the journal, and can be ordered from the ACS, and can be downloaded from the Internet; see any current masthead page for ordering information and Internet access instructions.

JA943576V

(54) Von Smoluchowski, M. *Z. Phys. Chem.* **1917**, *92*, 129.

(55) Kell, G. S. In *Water, a Comprehensive Treatise*; Franks, F., Ed.; Plenum Press: New York, 1972; Vol. 1.